Preparation and Characterization of Novel Hybrid of Bio-Assisted Mineralized Zn-Al Layered Double Hydroxides Using Chitosan As a Template

Dilip Depan,* Raj Pal Singh

Division of Polymer Science and Engineering, National Chemical Laboratory, Pune 411 008, India

Received 12 May 2007; accepted 10 September 2009
DOI 10.1002/app.31463
Published online 4 November 2009 in Wiley InterScience (www.interscience.wiley.com).

ABSTRACT: The purpose of this study was to prepare and characterize a novel nanohybrid prepared from the template-assisted mineralization of Zn-Al Layered Double Hydroxide (LDH) onto the surface of Chitosan (CSI), with an emphasis on morphology, biocompatibility, and its use as an efficient drug carrier agent. The as prepared LDH is highly crystalline, with platelet-like morphology and curved tactoids when nucleated onto the surface of CSI. Our results indicate that the —OH and —NH functional moieties on CSI can direct an ordered structure of LDH, due to the electrostatic interaction between biopolymer and inorganic lamellae. We have been successful to intercalate an anti-inflammatory drug, Sodium Ibuprofen (Ibu), into LDH, through conventional coprecipitation method. LDHs are endowed with great potential for delivery vector because their stacked layers lead to safe reservation of biofunctional molecules or genes, and their ion exchangeability and solubility in acidic media (pH < 4) give rise to the controlled release of drug molecules. According to the cell-growth studies, LDHs are found as cell viable up to the concentration of 500 μg/mL. This study reveals that LDH not only plays a role of a biocompatible-delivery matrix but also facilitates a significant increase in the delivery efficiency. © 2009 Wiley Periodicals, Inc. J Appl Polym Sci 115: 3636–3644, 2010

Key words: bio-assisted mineralization; chitosan; layered double hydroxides; drug delivery systems; cell-growth studies

INTRODUCTION

Molecular biomimetics or bio-assisted mineralization is the combination of physical and biological fields that leads to the formation of a variety of solid inorganic structures by living organisms, such as seashells, intracellular bone, teeth, algae, and also pathological biominerals such as gall and kidney stones.[1] Material scientists have shown ample interest for biomineralization process because the produced inorganic–organic hybrid shows interesting properties with a controlled morphological structure. In biominerals, the organic component exerts a reinforcing effect on the mechanical properties and expels the mineralization process to the formation of particles of well-defined size, novel crystal morphology, specific crystallographic orientation, and superb biological properties.[2] If we could even direct the use of biomaterials to mimic such mineralization processes, novel biofunctional materials that are environmentally benign could be designed with compositional control at the nanoscale level. There are few reports of mineralization and duplication of living bio-assembly by associating a biopolymer and a mineral, such as polylactide/layered silicate nanocomposites.[3] Moreover, according to recent studies, alginate–silica biocomposite can be used for enzyme and cell immobilization.[4]

Chitosan (CSI) [poly-β(1,4)-2-amino-2-deoxy-D-glucose] is a partially deacetylated derivative of chitin, a natural polymer found in the cell wall of fungi, microorganisms, and in mollusk shells, is believed to play an important role in controlling the mineralization process, *in vivo*.[5] The mineralization process mainly occurs through the following steps: (1) the biopolymer matrix forms a mineralization framework, where metallic ions are entrapped and associated through electrostatic interaction with soluble proteins/polysaccharides and adopts its shape; (2) subsequently, an oriented nuclei form across and the crystallization propagates from the surface of the matrix, resulting in the formation of a single crystal with controlled orientation and predetermined microstructure. Because of its properties, such as high mechanical strength, hydrophilicity, good adhesion, and nontoxicity, CSI is usually applied as food additive, as anticoagulant, or wound healing accelerator and permit its extensive use in the formulation

**Present address:* Faculty of Dentistry, McGill University, Montreal H3A 2B2, Canada.
Correspondence to: R. P. Singh (rp.singh@ncl.res.in).
Contract grant sponsors: University Grants Commission, New Delhi, India.

of a promising encapsulating agent in drug delivery systems.

Ibuprofen (Ibu) is a nonsteroidal anti-inflammatory (NSAID) drug used for the relief of rheumatoid arthritis, osteoarthritis, and is frequently used as a model drug for sustained release experiments because of its favorable molecular size, better pharmaceutical activity, and short biological halflife. Because of the frequent side effects, its use is often limited.[6] These problems could be reduced by a formulation able to control the drug release. As matrices to prepare a controlled release formulation, we have taken into account lamellar compounds. The idea was to store the drug in the interlayer region of the lamellar host and allow the drug release as a consequence of a diffusion-de-intercalation process.

Lamellar Layered Double Hydroxide (LDH) commonly called as synthetic anionic clays, whose structure is commonly described as edge-sharing octahedral sheets in which, by comparison with the Brucite M $(OH)_2$, some of the divalent cations are replaced by trivalent cations to give positively charged sheets. The excess charge is counter balanced by interlayer anions, leading to an anionic exchange capacity of 2.46 mq/g and associated with a layer charge density of 25.4 $Å^2$ per e^- for a ratio of 2 Zn to Al of 2. The general formula for LDH is $M^{+2}_{1-x}M^{+3}(OH)_2$. $(A^{n-})_{x/n}$. mH_2O, where M^{+2} is the divalent cation, M^{+3} is the trivalent cation, A^{n-} is the interlayer anion, and mH_2O refers to the water in the interlayer space. The interlayer anions can be exchanged with other negatively charged species such as drugs,[7] genes,[8] adenosine monophosphate,[9] and biopolymer such as poly (α, β-aspartate). In addition to that, LDH is biocompatible[10] and has found pharmaceutical applications as an antacid, which makes them promissory hosts for immobilization of NSAIDs aiming to reduce gastric irritation side effects.[11] Although gastric toxicity caused by these drugs can occur because of their acidic nature or cytotoxic effects in the induction of gastric lesions, it could be reduced by the immobilization of the drugs on an antacid host.

CSI has C=O, —OH, and —NH groups on its backbone that can coordinate strongly with the Lewis acidic sites (Zn^{+2} and Al^{+3} ions). This interaction is supposed to occur during the growth of LDH crystals, which can lead to specific size, control and morphology. We have intended to know how the biopolymer could direct an ordered structure with specific morphology and could orientate the assembly of inorganic lamellae. Moreover, CSI can provide the necessary controlled release and buffering property for the prepared nanohybrids to be used as an effective antacid. So, we choose to synthesize LDH/CSI hybrids by a coprecipitation route involving the *in situ* formation of LDH layers. Intercalation of Ibu was done by a conventional coprecipitation method. Here, CSI acts as a templating molecule for LDH crystallization, where CSI acts as a glue to consolidate nanosized LDH particles into larger scale aggregates. To the best of our knowledge, this is the first example of the preparation and physio-morphic investigation of Zn/Al layered double hydroxide using CSI as a template. The neutralizing and buffering capabilities of the nanohybrids in HCl aqueous solutions were also evaluated.

We envision that this novel system, which combines the advantages of both as an effective antacid and the property of controlled release, could play a significant role in the development of new generation, site specific, and sustained drug release.

EXPERIMENTAL

Materials and sample preparation

CSI (of low molecular weight, Mv 1.5×10^5, degree of deacetylation 85%, Sigma–Aldrich) was dissolved in an aqueous solution of lactic acid and NaOH was added to the biopolymer solution to reach a pH value of 9 to ensure complete deprotonation of carboxylic groups of CSI. Such a pH value is compatible with the standard coprecipitation of Zn-Al LDH as reported by de Roy et al.[12] Aqueous solutions of zinc and aluminum chloride were prepared from chemicals of analytical grades: $AlCl_3$ (>99%, Merck), $ZnCl_2$ (98%, Merck), NaOH (98%, S.D. Fine Chemicals). Deionized water (resistivity of 18.2 *M*Ω.cm) was obtained with a Millipore ultra pure water system was previously distilled and decarbonated by boiling and bubbling N_2. $AlCl_3$ (0.68 g) and 0.603 g of $ZnCl_2$ were dissolved in 500 mL of decarbonated bi-distilled water and added drop wise to the biopolymer solution under nitrogen atmosphere, to avoid the CO_3^{2-} contamination. The molar concentration of Zn^{2+} and Al^{3+} was taken as 1 mol/L, while maintaining a constant ratio of Zn/Al = 2.5. The aqueous solutions of Zn and Al were continuously added at the rate of 12 mL/h. The precipitate was aged in the mother liquid for 24 h, and the white solid products were isolated by repeated centrifuging and washing with decarbonated water and finally dried at 40°C. The pristine LDH without biopolymer, denoted as LDH was synthesized following the same procedure but replacing the biopolymer solution with bi-distilled water. During the centrifuging, sealed containers were used to avoid absorption of atmospheric carbon dioxide, and the deionized-bi-distilled water used for synthesis and washing was decarbonated before use by boiling and subsequent cooling in the absence of CO_2 by means of a gas-washing bottle filled with KOH solution.

Characterization techniques

Transmission electron microscopy (TEM) was carried with a JEOL 2000 EX-II instrument (JEOL, Tokyo, Japan) operated at an accelerating voltage of 100 kV. The Wide Angle X-ray Diffractometer patterns were obtained by Rigaku (Japan) X-Ray diffractometer with Cu-Kα radiation at 50 kV between the scan ranges of 2θ from 2° to 70° by the scan rate of 5°/min. The Fourier transform infrared (FTIR) spectra of the samples were obtained with a Perkin–Elmer Spectrum GX. Powder samples were molded in KBr pellets and analyzed at a resolution of 2 cm^{-1}. The internal structure and surface morphology was investigated by SEM (JEOL Stereoscan 440, Cambridge). ^{13}C-NMR ($I = 1/2$) and ^{27}Al ($I = 5/2$) CP MAS NMR spectra were obtained in a Bruker Avance 300 spectrometer, using a standard cross-polarization pulse sequence. Samples were spun at 10 kHz. The thermal gravimetric analysis (TGA) was conducted on a Perkin-Elmer TGA 7- thermal analyzer from 50 to 900°C with a heating rate of 10°C/min under nitrogen with flow rate of 20 mL/min.

Buffering capability, *in vitro* drug release, and cell-growth properties

Buffer capability

Buffering or neutralizing capability of the prepared nanohybrids was evaluated by monitoring the change in the pH value of the sample suspension with the addition of 0.1 mol/L HCl aqueous solution at 37°C. In a typical experiment, 100 mg of the prepared nanohybrids sample was suspended in a 10 mL of deionized water and kept stirring at 37°C. At a regular interval, aliquots of 0.1–0.5 mL of the HCl aqueous solution were added to the suspensions until the pH reached the value of ~ 1. This procedure was repeated until the entire solid was dissolved.

In vitro drug release

For *in vitro* drug release studies, Ibuprofen (Ibu) was taken as model drug. For this study, 1 g of LDH and CSI-LDH sample powder was added to 80 mL of a 5 m*M* aqueous Ibu drug solution at 60°C and stirred for 3 days. The Ibu was adsorbed onto the external surface of the LDH by surface adhesion method. The resulting Ibu loaded samples were dried under vacuum and washed thrice with hexane to remove any unadsorbed Ibu from the LDH surface. Release studies were performed by dispersing Ibu-LDH and CSI-Ibu-LDH in 200 mL Phosphate Buffer Saline (PBS, pH 6.8) at 37°C in the USP XX paddle type apparatus, and the Ibuprofen content (mass/volume ratio) was selected to simulate sink conditions, according to the Ibu solubility at this pH value.[13] Aliquots of 4 mL of dissolution medium were taken at different time interval, filtered with a 15 mm micro filter unit, and their Ibu content was determined by UV absorption at 264 nm. Fresh release media was replaced after every aliquot sample.

Cell-growth studies

The cell-growth studies were performed on HL-60 Leukemia Cell Line and the procedure was followed in accordance with the procedure suggested by Jae et al.[14] At 75–85% of confluence, test cells were trypsinized and plated at a density of 2.0×10^4 cells per well in the 96 well cell-culture plate. For this, after every 24 h, 100 μL of the cell culture was incubated for MTT assay and the absorbance was taken at 490 nm wavelength in Spectrophotometer Plate Reader.

All the *in vitro* tests were made in triplicate and the results were recorded as an average.

RESULTS AND DISCUSSION

XRD analysis

Figure 1 shows the powder XRD patterns of LDH and CSI-LDH. The d_{001} spacings are obtained by the first rational orders corresponding to the 001 reflections. The XRD pattern of LDH exhibits strong basal sharp set of (001) reflections, indicative of a long-range ordering in the stacking dimension. The first peak occurring at a low 2θ angle was attributed to the reflections from the (003) family of crystallographic planes, which equals the thickness of one brucite-like layers (approximately 4.8 Å) plus one interlayer repeat distance d (where $d = \lambda/2\sin\theta$). All the peaks were indexed in a hexagonal unit cell with R_3m rhombohedral symmetry, where $C_0 = 23.19$ Å, which corresponds to three times the distance between adjacent layers of interlayer distance of 7.73 Å, confirming the hydrotalcite-like material.[15] In addition, the sharp and symmetric features of the diffraction peaks reveal the high crystallinity, three-dimensional stacking order of the prepared LDH. The analogues peaks for the CSI-LDH are calculated from the d_{001} spacing and the thickness of the inorganic layers. LDHs crystallites grow faster in (110) plane rather than in (003) because of closer crystal plane distance of (110).[16] The average value of d_{003} for CSI-LDH is 13.96 Å. If the width of the brucite-like layer (4.8 Å)[17] is subtracted, the gallery height is 9.16 Å for the CSI- (the size of the CSI is 7.23 Å), somewhat smaller than the gallery height. This means that there is space enough to accommodate the biopolymer with its polysaccharide chain perpendicular to the layers in the interlayer, along with water molecules, even at high layer charge densities.

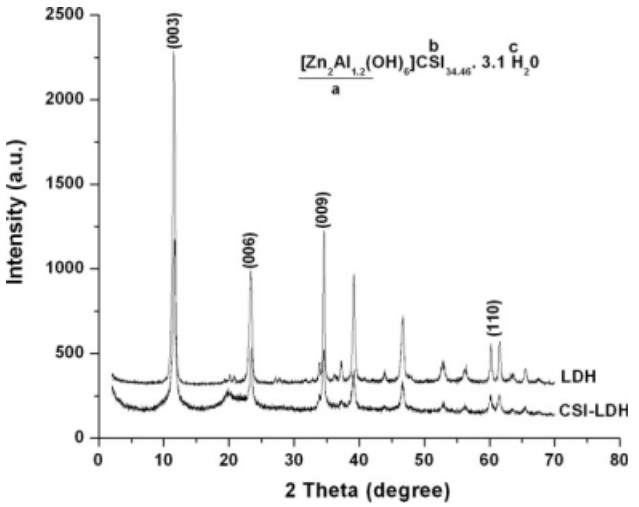

Figure 1 XRD pattern for LDH and CSI-LDH. The values given on the empirical formulae for CSI-LDH are derived from (a) Inductively Coupled Plasma-Atomic Emission Spectroscopy (ICP-AES), (b) CHN chemical analysis, and (c) TGA.

FTIR spectra

FTIR spectra of CSI, LDH, and CSI-LDH, in the range of 4000–400 cm^{-1}, are provided in Figure 2, which shows vibration bands at 1622 cm^{-1} (δ_{HOH}), 787 and 621 cm^{-1} ($\nu_{M\text{-}O}$), and a peak around 420 cm^{-1}, which is attributed to the $\delta_{O\text{-}M\text{-}O}$ deformation vibrations in the LDH sheets[18] indicating that the LDH structure is truly formed when CSI is used as a template, as confirmed previously by XRD. The peaks at 897 and 1152 cm^{-1} in CSI are assigned to the saccharine structures and a strong peak at 1597 cm^{-1} is due to strong amino group characteristic. A strong vibration band around 3450 cm^{-1} is observed in both the spectra of LDH and CSI-LDH and is attributed to the stretching vibration (ν_{OH}) of water molecules and hydroxyl groups belonging to brucite layers.[19] For CSI-LDH, the bands arising from various functionalities of CSI are located at their characteristic wave number bearing amino and acetyl groups (ν_{N-H} at $\sim$ 3450 cm^{-1}; ν_{O-H} $\sim$ 3362 cm^{-1},

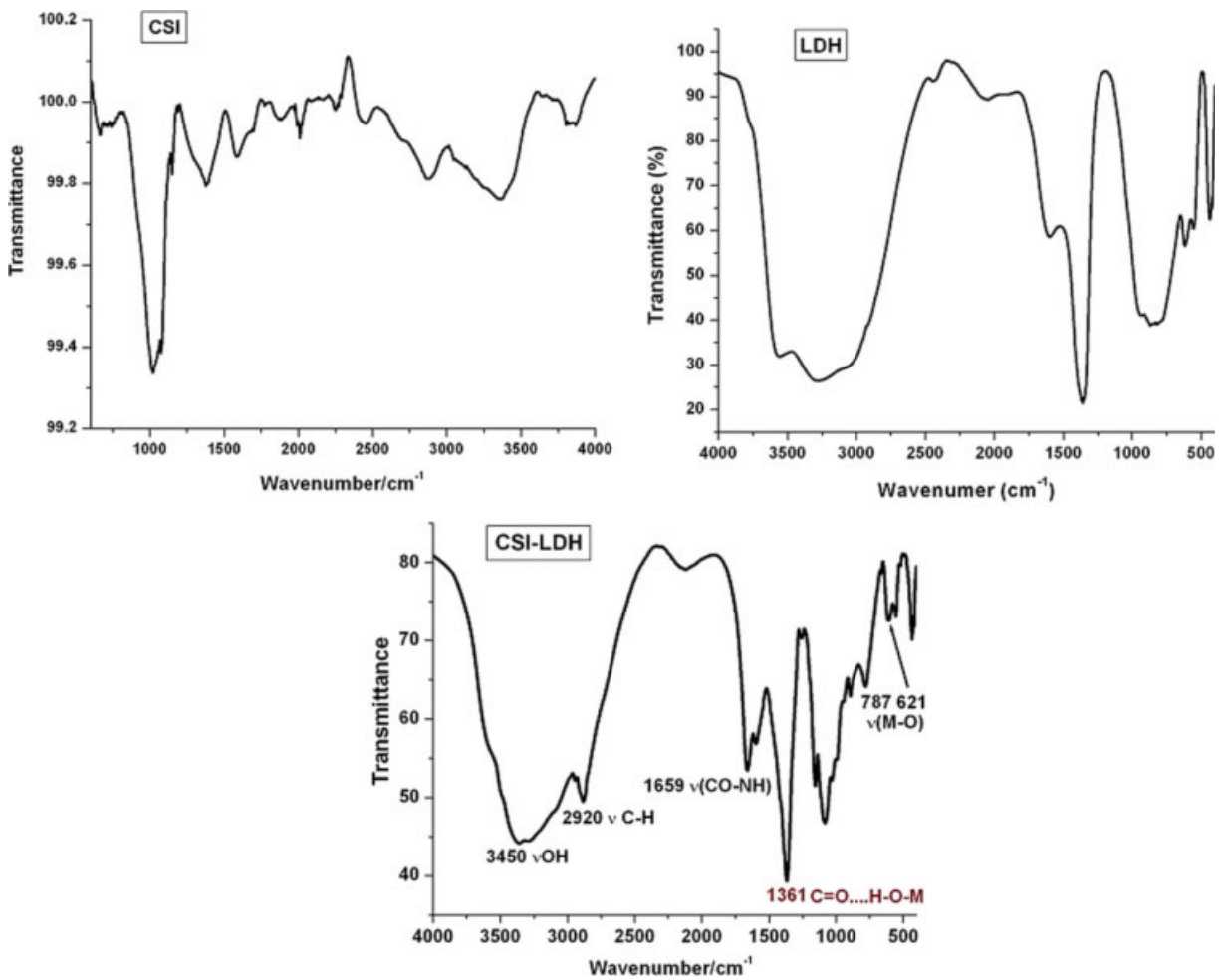

Figure 2 The FTIR spectra of prepared CSI, LDH, and CSI-LDH. [Color figure can be viewed in the online issue, which is available at www.interscience.wiley.com.]

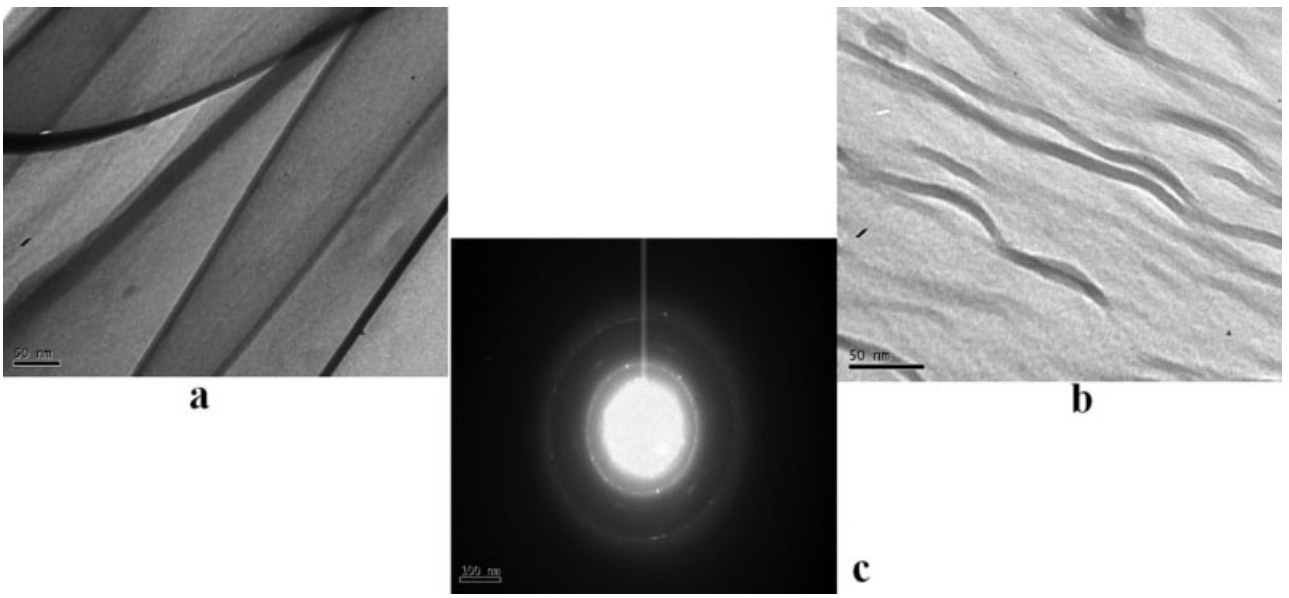

Figure 3 TEM images of (a) LDH, (b) CSI-LDH, and (c) Selected Area Electron Diffraction (SAED) pattern of CSI-LDH.

$\nu_{C-H} \sim 2920\ cm^{-1}$; amide II $\sim 1659\ cm^{-1}$; $\delta_{NH3} \sim 1597\ cm^{-1}$; δ_{CH}- $1320\ cm^{-1}$; ν_{C-O} of C—O—C $\sim 1152\ cm^{-1}$), characteristics of the pyranose ring.[20] The amide I band at $1650\ cm^{-1}$ is overlapped with δ_{HOH} bending vibrations at $1640\ cm^{-1}$ of the water molecules associated to the nanohybrids, as expected for a biopolymer with high water retention capacity. A downshift in frequency corresponding to a weakening of the C=O ($1361\ cm^{-1}$) bond strength is also observed. The disappearance of the C=O bond in CSI-LDH indicates the presence of an electrostatic binding with the anionic clay surface through a hydrogen bond via the path C=O···H—O—M (M = Zn or Al). It has been accepted that the coordination of the O atom in the CSI decreases the electron density in the C—O bond and thus also decreases the force constant in the vibration resulting the downward shift of the C—O vibration band to the lower wave number side, which has been observed in the FTIR spectra of CSI-LDH.

Microscopic measurement

TEM micrographs of LDH and CSI-LDH are given in Figure 3(a,b), respectively, which clearly shows the thin plate-like morphology of LDH having thickness of 30–40 nm and lateral dimension from 200 nm to 2 μm, whereas the TEM image of CSI-LDH show interesting curved tactoids with multiple layer agglomerates. He[21] and coworkers also observed similar morphology. Figure 3(c) shows the corresponding selected area electron diffraction (SAED) of CSI-LDH, which displays ring-patterns in agreement with the hexagonal-plate-like crystal structure with a crystallographic parameter a of 0.310 nm. These images are in good agreement with the XRD and SEM results. The SEM image of LDH [Fig. 4(a)] shows the usual "sand rose" morphology of the LDH, which is quite different from that observed in the SEM image of CSI-LDH [Fig. 4(b)]. The micro crystals of the CSI-LDH differ with the presence of large hexagonal chunks. The biopolymer seems to provide compactness to LDH, which results in the aggregation of the LDH particles. This is due to the strong edge-surface platelet interactions between inorganic LDH layers and the surface of the macromolecular biopolymer chains, respectively. Their corresponding CHN elemental analysis confirms the presence of C and N elements in the CSI-LDH samples, whereas Energy Dispersive X-ray analysis (EDAX) confirms the presence of Zn and Al in the prepared LDH nanohybrids, as shown in the EDAX analysis results.

Solid state NMR studies

Solid state CP-MAS ^{13}C-NMR is known to be very sensitive technique to evaluate the changes in the local structure and the chemical shifts of C-1 and C-4 carbon in 1, 4-linked carbohydrate, which is believed to be highly sensitive to any conformational change at the glycosidic linkage.[22] The resonance peaks for CSI are assigned according to the literature.[23] The signals observed on the spectra at 23.4 and 174.1 ppm were attributed to the signals of —CH_3 and —C=O of the glucosamine ring, respectively, (Fig. 5). These peaks in CSI-LDH show a slight shift, which is attributed to the electrostatic

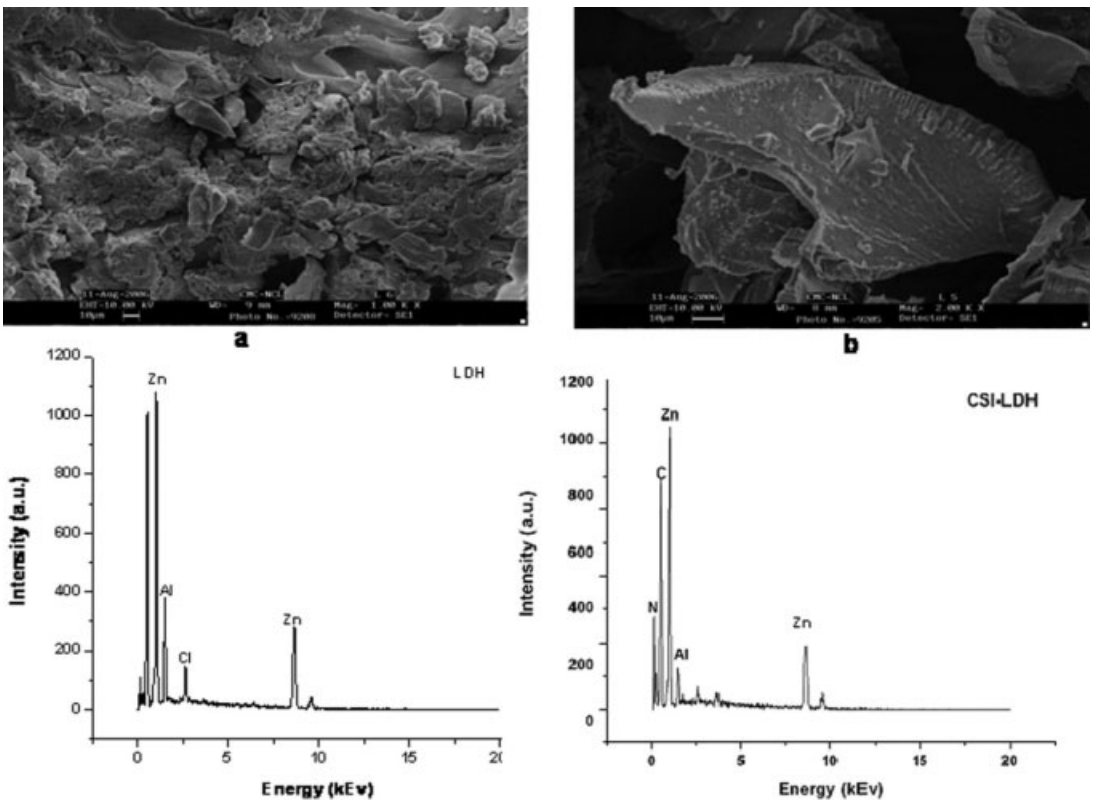

Figure 4 SEM images and their corresponding EDAX analysis results for (a) LDH and (b) CSI-LDH.

interaction between the biopolymer and positively charged Brucite layers, which is in qualitative agreement with the results obtained from TEM and FTIR. Similar results were also observed when other macromolecular guest species is intercalated into LDH.[24] We have unsuccessfully tried to confirm the nature of the components related to Al species from[25]-Al-NMR spectra but only a single signal around 13.2 ppm (Fig. 5, INSET), which corresponds to Al (III) in octahedral environment, appears in all the studied samples. The same type of signal is also observed in the LDH without CSI. EDAX analysis, along with ICP-AES, confirms the presence of elemental constituents of LDH and Zn/Al ratio for LDH and CSI-LDH as 1.87 and 2.1, respectively.

Thermal analysis

TG and DTG traces for CSI-LDH and LDH are shown in Figure 6(a,b), respectively. The shape of the curves reflects good crystallinity degree of the samples. LDH shows two mass loss events as evidenced by a curve with two well-differentiated regions. The first, corresponding to 15.5% weight loss between 50 and 210°C, has been attributed to elimination of both nongallery surface adsorbed water and interlayer water molecules. The second event, ~ 28% weight loss from 300 to 450°C, corresponds to the dehydroxylation and de-carbonation reactions of the Brucite layers.[26] The total mass loss, 43.5%, provides a water content of $n = 2.8$ based on complete conversion to the metal oxides, which agrees well with previous estimates of $n = 2$–4 for air-dried samples.[10] In contrast, three events are observed in the thermal trace obtained on the CSI-LDH. The first event, a 15% weight loss complete by around 100°C, should correspond to the elimination of adsorbed water at the surface and between LDH

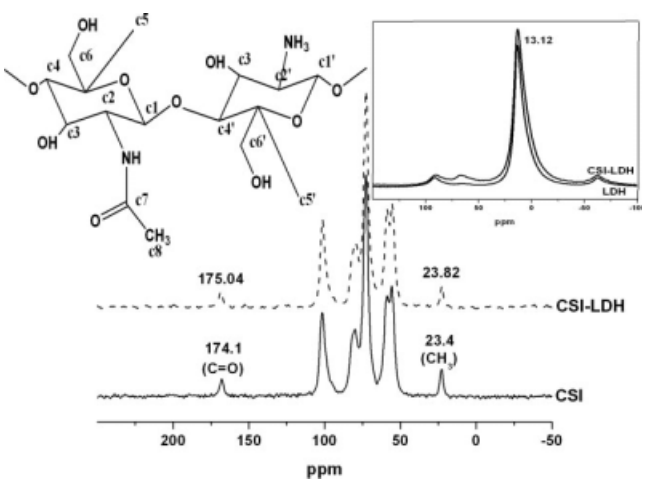

Figure 5 ^{13}C-NMR spectra of CSI and CSI-LDH. The INSET figure shows the[25]-Al NMR of the prepared LDH and CSI-LDH nanohybrids.

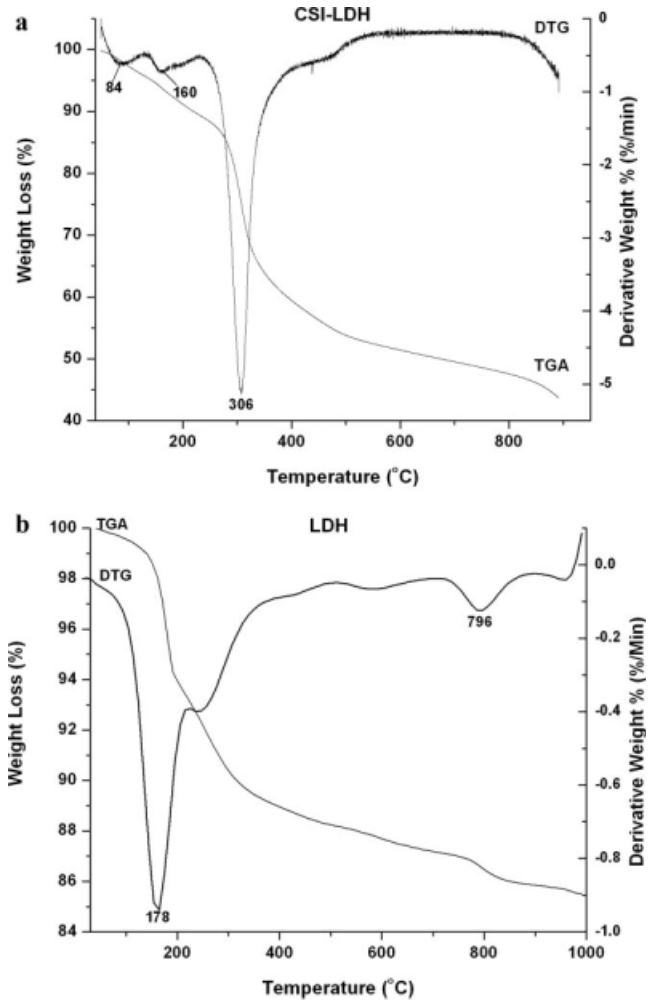

Figure 6 TGA and DTG Curves for the prepared (a) CSI-LDH and (b) TGA and DTG curves for LDH nanohybrids.

layers. A second weight loss from 300 to 500°C (23%) is ascribed to the dehydroxylation of the LDH layers and partial decomposition of the CSI biopolymer. The final mass loss is observed at ~ 800°C (22%) and is ascribed to complete oxidative elimination of the carbonaceous residue derived from the initial biopolymer degradation.

In vitro release studies

Buffer Capability

Buffering effects of the prepared nanohybrids were evaluated by monitoring the changes on the pH values by subsequent addition of HCl into the perspective aqueous solutions of the Ibu-LDH and CSI-Ibu-LDH. The correspondent calibration graphs for the evaluation of buffer capability of the prepared nanohybrids are given in Figure 7(a,b). Ibu-LDH shows buffering effect by keeping the pH constant at 3.9 after an addition of 19 mL of HCl, whereas CSI-Ibu-LDH shows slightly more buffering activity due to the alkaline nature of CSI that can effectively neutralize the added HCl.

The neutralizing and buffering capabilities of the nanohybrids are due to the —OH and CO_3^{2-} moieties located in the interlayer and on external surface of the LDH. Moreover, CSI has $—NH_2$ groups that can acts as a neutralizing agent to the acid and hence works as an effective antacid.

Cell-growth studies

LDH and CSI-LDH were found to be nontoxic, even at a higher concentration of 500 μg/mL of the nanohybrids, as evidenced by cell-growth studies as shown in Figure 7(c). The cell growth was measured by MTT assay of HL-60 leukemia cell-line cultures on the prepared samples. The growth of cells cultured is higher on first day, while it decreases with increasing time duration. It is possibly because, during proliferation, cells may have occupied all the available spaces on the specimens. LDH and CSI-LDH did not show significant difference in the cell growth. The lamellar host, in this study, is layered double hydroxides, which are composed of thin-stacked lamellae of Zn and Al hydroxides that are combined with rather weak interaction such as Vander walls force and H-bonding. The interaction between the host (stacked lamellae) and guest (biopolymer and drug) compounds can offer an opportunity to develop various new hybrid compounds for pharmaceutical use. We postulate that LDH may develop London-Vander Valls forces and hydrogen bonding with the cells. As the biopolymer matrix is incorporated with LDH, the biopolymer would be surrounded and/or adsorbed onto LDH layers, which can act as an adhesive between the biopolymer and the cells through hydrogen bonding between the hydroxyl groups of CSI and the water of hydration on LDH. Moreover, under acidic environment (pH 4–5) of cytoplasm, LDH disintegrates into Zn and Al ions that are cell friendly and does not impart any toxic effects, even at a higher concentration, as proposed in the present study. Similar results were also observed by Kriven et al.[27]

In vitro release studies

Figure 8 shows the *in vitro* drug release profile of the prepared Ibu loaded nanohybrids. For Ibu-LDH, 60% of the drug was released after 20 min and 100% after 110 min, whereas for CSI-Ibu-LDH, it was 30% drug release after 20 min and 100% after 110 min, when immersed in the release media. The reason behind this sustained release behavior is that the interlayer region of CSI-LDH matrix acts like a micro vessel in which the incorporated drug molecules can be released by a diffusion-deintercalation process

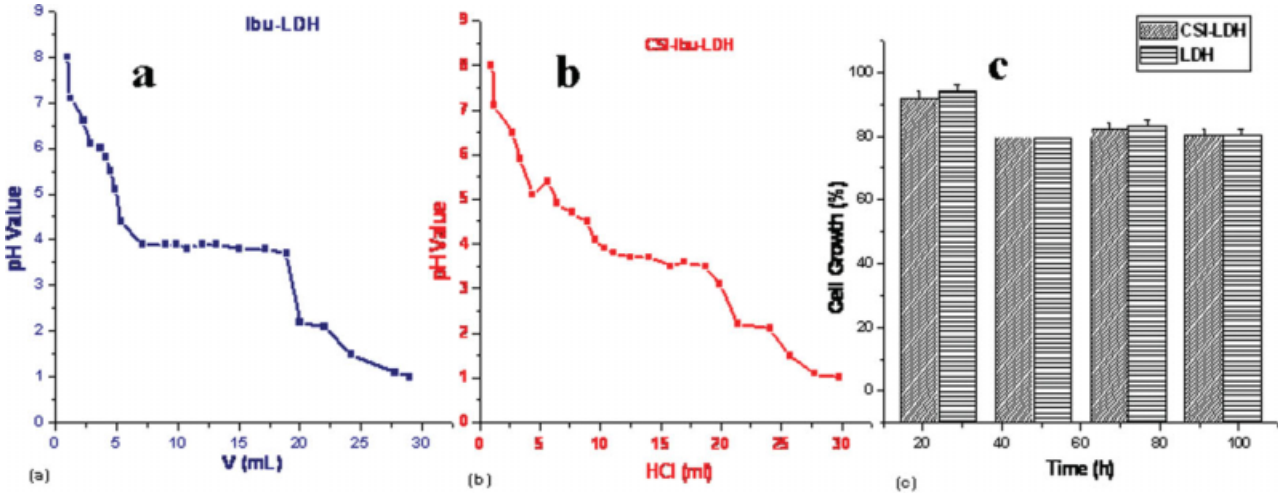

Figure 7 Buffer capability of (a) Ibu-LDH, (b) CSI-Ibu-LDH, and (c) Cell-Growth studies. The final concentration for the Cell-Growth Studies of the nanohybrids was 500 μg/mL. [Color figure can be viewed in the online issue, which is available at www.interscience.wiley.com.]

triggered by an ion exchange method, due to the ions already present in the phosphate buffer saline (PBS) of the release media. This fluid is having the same pH and ionic concentration of small intestine. When LDH is dispersed in PBS solution, phosphate ions (small anionic species) of the release media will be in the close proximity of stacked lamellae of LDH and are more prone for an ion exchange process with the already present ions (Sodium Ibuprofen drug molecules) of LDH.[25] In the case of LDH, $H_2PO_4^-$ anions, once exchanged with the Ibu ions, react with the interlayer —OH groups of LDH to form layered hydroxyphosphates by a grafting reaction. In this condition, the phosphates are no longer exchangeable and can obstruct the exit of intercalated Ibu, as suggested by Ambrogi et al.[28] As Ibu anions do not pass through the matrix directly, neither can pass over the grafted anions, they have to find the right pathway with consequent increase of the tortuosity and the length of the diffusion pathway in the limited and confined space. The effect of incorporation of LDH layers can be significantly found as reduced rate of release at initial stage of immersion for both Ibu-LDH and CSI-Ibu-LDH. During initial stage of immersion (up to 25 min), the specimen is solvated, which facilitates the lateral diffusion of drugs. After 40–50 min, the rate of release is moderate and sustained over the time. This may be due to the interactions of LDH layers and CSI biopolymer chains with the loaded drug molecules. The interaction between the sodium salt of Ibuprofen and LDH surface is stable enough to exhibit the sustained release profile. In many pharmaceutical uses, drugs are exposed to various body fluids, such as blood, serum, and cytosol, which have a high concentration of salts and polyelectrolytes like proteins. In such conditions, the nontoxic minerals like LDH, which are ionic in nature, can flocculate with polyelectrolytes on the surface. Moreover, the presence of CSI results in the formation of the neutral biopolymer matrix on the surface that is advantageous for the improvement of its dispersion stability and bioavailability. This sustained release profile offers a great interest for pharmaceutical application to achieve therapeutic efficacy and rapid delivery profile of poorly water-soluble drugs like Ibuprofen.

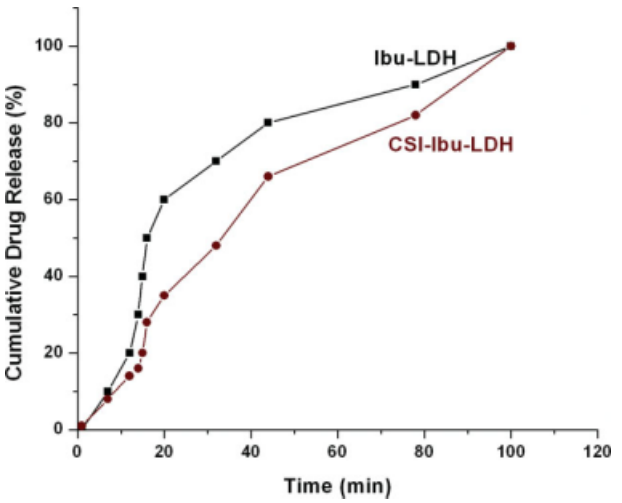

Figure 8 Cumulative drug release profiles for Ibu-LDH and CSI-Ibu-LDH nanohybrids. [Color figure can be viewed in the online issue, which is available at www.interscience.wiley.com.]

CONCLUSIONS

In summary, this investigation provided evidence for the feasibility of bio-assisted mineralization of

LDH onto CSI, with novel physio-morphic and biophysical properties, with an optimized route to avoid contamination by atmospheric carbon dioxide. XRD pattern of the nanohybrids indicates the formation of highly crystallized hydrotalcite-like phase. The buffer capability of the prepared nanohybrids in the pH range 3.6 seems to be ideal for the application as an effective antacid. The Ibu drug-release studies showed that the drug release was better controlled for CSI-LDH. Our CSI-LDH nano hybrid approach represents a novel way to synthesize highly crystalline LDH, which can be used as inorganic carriers able to intercalate drugs and release them by a diffusion-de-intercalation process and to prepare a controlled release formulation.

The authors are grateful to Dr. S. Sivaram, Director, National Chemical Laboratory, Pune, India.

References

1. Mann, S. Biomineralization; Oxford University Press: Oxford, 2001; p 198.
2. Smith, B.; Schaffer, T.; Viani, M.; Thompson, J.; Frederick, N.; Kindt, J.; Belcher, A.; Stucky, G.; Morse, D.; Hansma, P. Nature 1999, 399, 761.
3. Maiti, P.; Yamada, K.; Okamoto, M.; Ueda, K.; Okamoto, K. Chem Mater 2002, 14, 4654.
4. Coradin, T.; Mercey, E.; Lisnard, L.; Lirage, J. Chem Commun 2001, 2496.
5. Falini, G. Tissue Eng 2004, 10, 1.
6. Griffin, M.; Sheiman, J. Am J Med 2001, 110, S33.
7. Zhang, H.; Zou, K.; Guo, S.; Duan, X. J Solid State Chem 2006, 179, 1792.
8. Tyner, K.-M.; Roberson, M.-S.; Berghor, A.; Li, L.; Gilmonr, R.-F., Jr.; Batt, C.-A.; Giannelis, E.-P. J Controlled Release 2004, 100, 399.
9. Choy, J.-H.; Kwak, S.-Y.; Park, J.-S.; Jeong, Y.-J. J Mater Chem 2001, 11, 1671.
10. Cavani, F.; Trifiro, F.; Vaccari, A.; Catal Today 1991, 11, 173.
11. Goodman-Gilman, A.; Goodman, L.-S.; Goodman, A. The Pharmacological Basis of Therapeutics, VI. Macmillan Publishing Co. Inc.: New York, 1975; p 995.
12. Roy, A. de.; Forano, C.; Maiki, M.-El.; Besse, J.-P. In Synthesis of Microporous Materials, Expanded Clays and other Microporous Solids; Occelli, M. L., Robson, H. E., Eds.; Van Nostrand Reinhold: New York, 1992; p 108.
13. Adeyeye, C.-M.; Price, J.-C. J Microencapsul 1997, 14, 357.
14. Jae, M.-O.; Man, P.; Sang-Tae, K.; Jin-Young, J.; Yong-Gu, K.; Choy J.-H. J Phys Chem Solids 2006, 67, 1024.
15. Miyata, S. Clays Clay Miner 1975, 23, 369.
16. Zhao, Y.; He, J.; Jiao, Q. Z.; Evans, D. G.; Duan, X. Chin J Inorg Chem 2001, 17, 573.
17. Kwon, T.; Tsigdinos, G.-A.; Pinnavaia, T. J. J Am Chem Soc 1998, 110, 3653.
18. Kooli, F.; Depege, C.; Ennaqadi, A.; Besse J.–P. Clays Clay Miner 1997, 45, 92.
19. Kloprogge, J.-T.; Frost, R. L. In Layered Double Hydroxides: Preset and Future; Rives, V., Ed.; Nova Science Publishers: New York, 2001; Chapter 5, p 139.
20. Depan, D.; Singh, R.-P. J Biomed Mater Res Part A 2006, 78, 372.
21. Li, B.; He, J.; Evans, D.-G.; Duan, X. J Phys Chem Solids 2006, 67, 1067.
22. Tanner, S.; Chanzy, H.; Vicendon, M.; Roux, J.-C.; Gaill, F. Macromol 1990, 23, 3576.
23. Cervera, M.-F.; Heinamaki, J.; Rasanen, M.; Maunu, S.-L.; Karjalainen, M.; Acosta, O. M. N.; Colarte, A. I.; Yliruusi, J. Carbo Polym 2004, 58, 401.
24. Messermith, P. B.; Stupp, S.-I. Chem Mater 1995, 7, 454.
25. Tammaro, L.; Constantino, U.; Bolognese, A.; Sammartino, G.; Marenzi, G.; Calignano, A.; Tete, S.; Mastrangelo, S.; Califano, L.; Vittoria, V. Int J Antimicrob Agents 2007, 29, 417.
26. Constantino, V. R. L.; Pinnavaia, T. J. Inorg Chem 1995, 34, 883.
27. Kriven, W.-M.; Kwak, S.-Y.; Kriven, W.-M.; Wallig, M.-A.; Choy, J.-H. Biomaterials 2004, 25, 5995.
28. Ambrogi, V.; Fardella, G.; Grandolini, G.; Perioli L. Int J Pharma 2001, 220, 23.